AIP | Applied Physics Letters

The effects of charge injection in single-wall carbon nanotubes studied by charge-induced absorption

W. Joshua Kennedy and Z. Valy Vardeny

Citation: Appl. Phys. Lett. **98**, 263110 (2011); doi: 10.1063/1.3606382
View online: http://dx.doi.org/10.1063/1.3606382
View Table of Contents: http://apl.aip.org/resource/1/APPLAB/v98/i26
Published by the American Institute of Physics.

The effects of charge injection in single-wall carbon nanotubes studied by charge-induced absorption

W. Joshua Kennedy[a] and Z. Valy Vardeny
Department of Physics and Astronomy, University of Utah, Salt Lake City, Utah 84112-0830, USA

(Received 31 March 2011; accepted 10 June 2011; published online 29 June 2011)

We studied direct charge injection in a heterogeneous film of single-wall carbon nanotubes using the technique of charge-induced absorption. We found that the injected charges screen the excitons in the semiconducting tubes, reducing their binding energy and transferring oscillator strength from the exciton transitions to free carriers. These effects parallel those of the electrochemical doping in the same samples. © *2011 American Institute of Physics*. [doi:10.1063/1.3606382]

The unique physical and optoelectronic properties of single-wall carbon nanotubes (SWNTs) make them ideal for many potential technological applications. Many proposed electronic devices that may take advantage of these properties depend on the nature of charge injection into, and transport through, the nanotubes.[1,2] Such devices include SWNT transistors and diodes,[3] chemical sensors,[4] nano-scale actuators,[5,6] infrared-transparent conducting films,[7,8] and polymer-nanotube composites for use in organic photovoltaic cells and light-emitting diodes.[9] Many such applications involve changing the electronic properties of nanotubes via contact with an external gating mechanism, direct ion doping, electrochemical doping, or other similar mechanism. Spectroscopic studies of the optically active exciton transitions in single-wall nanotubes are powerful tools for exploring their electronic interactions, even in samples composed of a variety of nanotube species; there have been many investigations into the spectroscopic effects of gated and doped nanotubes.[7,8,10–13]

A complete understanding of the effects on absorption by the injected charges in single-wall carbon nanotubes is necessary to realize the many potential technological applications that have been envisioned. Charge-induced absorption (CIA) is a technique that directly probes the effects of charge injection on the optical response of a device. It is complementary to electroabsorption in that the sample resistance and modulation frequency are low, allowing charges to be injected into the device rather than placing an electric field across the device. CIA has been used to study various types of injected carriers in organic semiconductors, specifically to observe their direct spectroscopic signatures.[14,15] In this letter, we report studies of the optical response of a heterogeneous film of SWNTs using CIA and compare it to the changes in absorption observed in electrochemically doped nanotubes.

We constructed a device for injecting charges into a nanotube film by depositing a semi-transparent layer of aluminum or ITO onto a sapphire substrate. An aqueous suspension of purified, single-wall carbon nanotubes dispersed with sodium dodecyl sulfate (SDS) was then drop-cast to an average thickness of 0.5 μm. A second layer of aluminum of approximately 200 nm thick was deposited on the top to complete the device.

The electrode layers were offset so as to avoid potential short-circuits and to provide easy electrical contacts as shown in Figure 1(a). A potential difference of up to 10 V was applied between the two electrodes via a sinusoidal signal generator at a frequency of 300 Hz. A white light, provided by an incandescent tungsten-halogen lamp, passed through the substrate, transparent electrode, and nanotube film and was reflected off of the thicker electrode layer at the other side (see Figures 1(b) and 1(c)). The light was then dispersed with a 1/4-m monochromator, and the signal at the photodetector was analyzed using a digital lock-in amplifier synchronized to the modulation frequency of the voltage generator. The SDS partially encases the nanotubes, reducing the average size of the naturally occurring bundles. The nanotubes fully percolate the film, however, and the surfactant is optically inert.

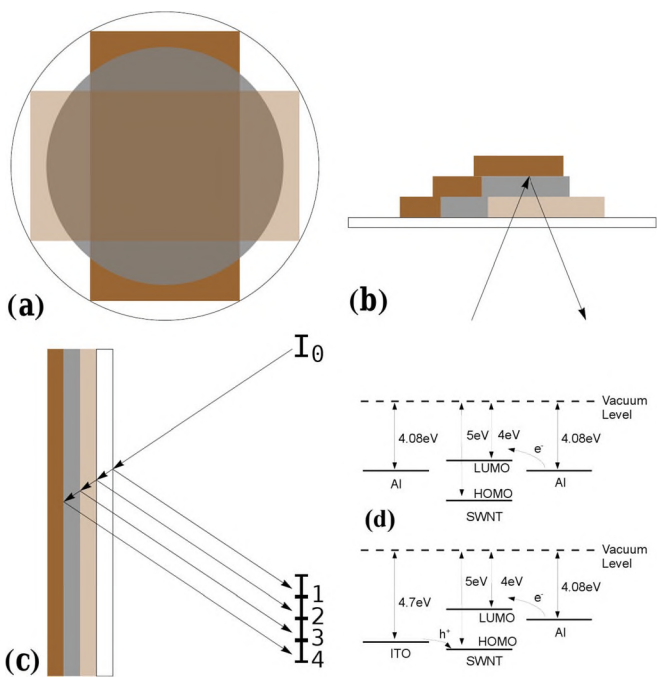

FIG. 1. (Color online) The CIA device. (a) A top view of the device showing the cross-orientation of the electrodes with the circular nanotube film between. (b) A side view showing both electrodes in contact with the sapphire substrate and open for contact from above. (c) A detailed diagram of the light signal at the detector. (d) A schematic of the electron energy levels for unipolar (upper) and bipolar (lower) devices.

[a]Electronic mail: w.joshua.kennedy@gmail.com.

The charge injection into the nanotube film depends on the work function of each electrode and the electron energy levels within the nanotubes. The average highest occupied molecular orbital (HOMO) for SWNTs lies approximately 5 eV below the vacuum level,[16] and the average distance between the ground state and the lowest unoccupied molecular orbital (LUMO) in our sample is around 1 eV. Therefore, aluminum electrodes primarily inject electrons into empty LUMO states, while ITO primarily accepts electrons from the HOMO states as shown in Figure 1(d).

The inherent inhomogeneity of our nanotube films makes it necessary to deposit a thick top electrode for good electrical contact. Therefore, additional data and analysis are required to determine the change in absorption due to the injected charges. Figure 1(c) shows a simplified diagram of the light rays involved in our experiment. Since the reflection at each intermediate surface is small compared to the reflection at the top electrode, we will ignore the effects of secondary reflections. In this same order of approximation, only the nanotube film contributes any significant absorbance.

The total signal at the detector comprises the reflected beams from the substrate I_1, the transparent electrode I_2, the nanotube film I_3, and the opaque electrode I_4. In general, these intensities are a function of ω, the frequency of the incident light. The reflected light from the front side of the substrate has intensity $I_1(\omega) = r_1(\omega)I_0(\omega)$. Subsequently, the reflected light at each surface depends on the light transmitted through the previous layers. Additionally, the nanotubes absorb some of the light as it passes through the film both before and after reflecting off of the top electrode. Therefore, $I_4 = r_4(I_0 - I_1 - I_2 - I_3)\exp(-2\alpha d)$, where d is the thickness of the film and α is the absorption coefficient. The charge-induced changes in optical density $\Delta OD = \Delta(\alpha d)$ are calculated as a function of the CIA signal ΔI, the reflection coefficients at each interface, and the unperturbed absorption of the film using the following *Ansatz*:

$$\Delta I = \Delta(I_1 + I_2 + I_3 + I_4) = \Delta I_4 \tag{1}$$

$$= \Delta[(1 - r_1)^2(1 - r_2)^2(1 - r_3)^2 r_4 e^{-2\alpha d}] \tag{2}$$

$$\approx -(2d\Delta\alpha)[\tilde{r}e^{-2\alpha d}] \tag{3}$$

$$\Delta OD = \frac{\Delta I}{2[\tilde{r}e^{-2\alpha d}]} \tag{4}$$

where we have made the substitution $\tilde{r} = (1 - r_1)^2 (1 - r_2)^2(1 - r_3)^2 r_4$.

We measured the absorption of our film using a spectrophotometer in the visible and near-infrared and a Fourier-transform infrared spectrometer in the mid- and far-infrared. We also directly measured the reflectivity of each surface in our device with the same two instruments by obtaining reflectivity spectra at each step of the manufacturing process.

For comparison, we also measured the absorption of our film after electrochemical doping (ECD) in 1 M aqueous solution of sodium chloride (NaCl) at a potential of 1 V relative to a silver/silver chloride reference electrode. For these measurements, a film was deposited on a sapphire substrate without the device electrodes, and a separate electrical contact was made outside of the cell to a platinum electrode. The sample was charged for approximately 5 min and then removed from the cell, rinsed with de-ionized water, and dried under flowing nitrogen. The absorption spectrum was then obtained within the next few minutes. Details have been reported elsewhere.[17]

A typical CIA spectrum for our device at 9 V bias is shown in Figure 2(a). The solid curve corresponds to a unipolar device and the dashed curve corresponds to a bipolar device. There is pronounced bleaching of the absorption between 0.6 eV and 1.6 eV as well as above 1.8 eV. There is little or no change in the absorption in the small portions of the spectrum around 0.5 eV and 1.7 eV. Between 0.49 eV and 0.55 eV, the charge-induced absorption is essentially zero (the "isosbestic point"), whereas, below 0.49 eV, there is an enhanced absorption. For comparison, Figure 2(b) shows the change in optical density of the nanotube film after ECD. Figure 2(c) shows the voltage dependence of the CIA signal for three different photon energies. The positive and negative CIA magnitudes increase with increasing applied voltage up to 8 V, above which the CIA saturates. Figure 2(d) shows the I-V characteristic of the bipolar device.

ECD of the nanotube film results in a bleaching of the exciton transitions in semiconducting tubes due to k-space filling and band-gap renormalization, but there is little effect on the lowest energy metallic transitions.[18–20] This is shown clearly in Figure 2(b) where there is pronounced bleaching in the S_{11} and S_{22} excitons. The overall negative offset is due primarily to a doping-induced shift in the π-plasmon background due to changes in intertube interactions because of the physical presence of the doping ions. The general effect of direct charge injection is similar, but the features in the

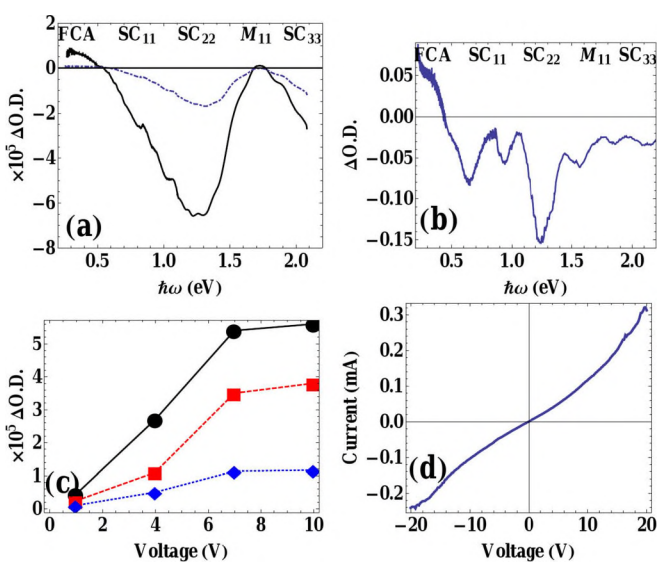

FIG. 2. (Color online) CIA spectra shown with ECD results. (a) The CIA spectrum from 0.21 eV to 2.1 eV. The signal for the unipolar (solid black) and bipolar (dashed blue) devices are shown. (b) The ECD induced changes to absorption over the same range. (c) The voltage dependence of the magnitude of the CIA signal at three places in the spectrum: 1.5 eV (black circles), 0.7 eV (red squares), and 0.35 eV (blue diamonds). (d) A typical IV curve for the device.

CIA spectrum are far less distinct than those in the ECD spectrum, and the absence of any CIA signal from the metallic tubes is even more noticeable because there is no overall shift from the π-plasmon. Thus, the CIA technique distinguishes between charging effects and effects due to the presence of the dopant in the nanotube environment.

We used the radial breathing mode energies from the Raman spectra to confirm the manufacturer's specification that the average nanotube diameter in our sample is approximately 1.2 nm. Thus, the lowest two semiconducting excitons have energies of roughly 0.6 eV and 1.3 eV respectively.[21] This also corresponds well with the observed absorption peaks in our film. The lowest excitonic transition for metallic tubes of the same average diameter is at 1.7 eV. Thus, we conclude that the only nanotubes whose absorption is bleached by the injection of charges in our device are the semiconducting tubes in our film. A likely explanation for this phenomenon is that exciton transitions in the metallic nanotubes are already partially screened by the existing free carriers, so that the additional screening by the injected carriers is too small to be detected by CIA. In other words, because of the large, flat density of states near the Fermi level in metallic tubes, neither electrochemically induced charges nor directly injected charges can move the Fermi level significantly.

The small features in the CIA spectrum such as those near 0.85 eV, 1.1 eV, and 1.25 eV (see Figure 2(a)) may reflect the distribution of certain semiconducting species that retain more of the injected charges. They may be farther from any metallic neighbors or the differences may be due to intrinsic differences in the carrier injection barriers for different types of tubes. The saturation of the CIA signal at large bias voltages (large currents) may be an indication of a change in the injection mechanism. As seen in Figure 2(c), the voltage dependence of the CIA signal is similar in each region of the spectrum. It is possible that metallic tubes begin to dominate the conduction above 8 V, thereby suppressing further charge injection into the semiconducting tubes. Alternatively, the semiconducting contacts themselves may become more Ohmic at that point.

In conclusion, we have observed the charge-induced bleaching of excitonic transitions in semiconducting nanotubes along with a simultaneous enhancement of the infrared absorption from free carriers. There is a non-Ohmic charge injection into the semiconducting tubes resulting in an increased exciton screening by the additional charges, while there is no shift in the plasmon absorption background and no bleaching of the metallic transitions in the same sample. Each of these effects is larger in unipolar devices than in bipolar devices due to the lack of electron-hole recombination in unipolar devices.

We thank Dr. Tho Nguyen for his suggestions and insight and for his help with the CIA measurements. This work was supported in part by the DOE Grant No. DE-FG02-04ER46109 and NSF Grant No. DMR 08-03325 at the University of Utah.

[1]P. Avouris, Z. Chen, and V. Perebeinos, Nat. Nanotechnol. **2**, 605 (2007).
[2]M. P. Anantram and F. Leonard, Rep. Prog. Phys. **69**, 507 (2006).
[3]N. Gabor, Z. Zhong, K. Bosnick, J. Park, and P. McEuen, Science **325**, 1367 (2009).
[4]A. Salehi-Khojin, C. Field, J. Yeom, and R. Masel, Appl. Phys. Lett. **96**, 163110 (2010).
[5]B. Lassagne, Y. Tarakanov, J. Kinaret, D. Garcia-Sanchez, and A. Bachtold, Science **325**, 1107 (2009).
[6]R. Baughman, C. Cui, A. Zakhidov, Z. Iqbal, J. Marisci, G. Spinks, G. Wallace, A. Mazzoldi, D. D. Rossi, A. Rinzler, O. Jaschinski, S. Roth, and M. Kertesz, Science **284**, 1340 (1999).
[7]L. Hu, D. Hecht, and G. Gruner, Appl. Phys. Lett. **94**, 081103 (2009).
[8]Z. Wu, Z. Vhen, X. Du, J. Logan, J. Sippel, M. Nikolou, K. Kamaras, J. Reynolds, D. Tanner, A. Hebard, and A. Rinzler, Science **305**, 1273 (2004).
[9]G. Safar, H. Ribeiro, C. Fantini, F. O. Plentz, A. Santos, G. DeFreitas-Silfa, and Y. Idemon, Carbon **48**, 377 (2010).
[10]M. Steiner, M. Freitag, V. Perebeinos, A. Naumov, J. Small, and P. A. A. Bol, Nano Lett. **9**, 3477 (2009).
[11]R. Jacquemin, S. Kazaoui, D. Yu, N. Minami, H. Kataura, and Y. Achiba, Synth. Met. **115**, 283 (2000).
[12]G. Luo, J. Zheng, J. Lu, W.-N. Mei, L. Wang, L. Lai, J. Zhou, R. Qin, H. Li, and Z. Gao, J. Phys. Chem. C **113**, 7058 (2009).
[13]K. Moonoosawmy and P. Kruse, J. Am. Chem. Soc. **132**, 1572 (2010).
[14]T. Nguyen, J. Rybicki, Y. Sheng, and M. Wohlgenannt, Phys. Rev. B **77**, 035210 (2008).
[15]T. Rabe, P. Gorrn, M. Lehnhardt, M. Tilgner, T. Riedl, and W. Kowalsky, Phys. Rev. Lett. **102**, 137401 (2009).
[16]M. Shiraishi and M. Ata, Carbon **39**, 1913 (2001).
[17]W. J. Kennedy, *Optical and vibrational properties of single-wall carbon nanotubes*. Ph.D. thesis (University of Utah, 2011).
[18]Z. Wu, Z. Chen, X. Du, J. Logan, J. Sippel, M. Nikolou, K. Kamaras, J. Reynolds, D. Tanner, A. Hebard, and A. Rinzler, Science **305**, 1273 (2004).
[19]A. G. Walsh, A. N. Vamivakas, Y. Yin, S. B. Cronin, M. S. Unlu, B. B. Goldberg, and A. K. Swan, Nano Lett. **7**, 1485 (2007).
[20]O. Kimizuka, O. Tanaike, J. Yamashita, T. Hiraoka, D. N. Futaba, K. Hata, K. Machida, S. Suematsu, K. Tamamitsu, S. Saeki, Y. Yamada, and H. Hatori, Carbon **46**, 1999 (2008).
[21]S. M. Bachilo, M. S. Strano, C. Kittrell, R. H. Hauge, R. E. Smalley, and R. B. Weisman, Science **298**, 2361 (2002).